An Updated Analysis of Clad Degradation

Spent Fuel and Waste Disposition

Prepared for
US Department of Energy
Spent Fuel and Waste Science and Technology
Patrick V. Brady and Brady D. Hanson
Sandia National Laboratories and
Pacific Northwest National Laboratory

November 19, 2020
M3SF-20SN010305111
SAND2020-13018 R

DISCLAIMER

This information was prepared as an account of work sponsored by an agency of the U.S. Government. Neither the U.S. Government nor any agency thereof, nor any of their employees, makes any warranty, expressed or implied, or assumes any legal liability or responsibility for the accuracy, completeness, or usefulness, of any information, apparatus, product, or process disclosed, or represents that its use would not infringe privately owned rights. References herein to any specific commercial product, process, or service by trade name, trade mark, manufacturer, or otherwise, does not necessarily constitute or imply its endorsement, recommendation, or favoring by the U.S. Government or any agency thereof. The views and opinions of authors expressed herein do not necessarily state or reflect those of the U.S. Government or any agency thereof.

This is a technical document that does not take into account contractual limitations or obligations under the Standard Contract for Disposal of Spent Nuclear Fuel and/or High-Level Radioactive Waste (Standard Contract) (10 CFR Part 961) For example, under the provisions of the Standard Contract, spent nuclear fuel in multi-assembly canisters is not an acceptable waste form, absent a mutually agreed to contract amendment.

To the extent discussions or recommendations in this document conflict with the provisions of the Standard Contract, the Standard Contract governs the obligations of the parties, and this document in no manner supersedes, overrides, or amends the Standard Contract.

This document reflects technical work which could support future decision making by DOE. No inferences should be drawn from this document regarding future actions by DOE, which are limited both by the terms of the Standard Contract and Congressional appropriations for the Department to fulfill its obligations under the Nuclear Waste Policy Act including licensing and construction of a spent nuclear fuel repository.

Sandia National Laboratories is a multimission laboratory managed and operated by National Technology & Engineering Solutions of Sandia, LLC, a wholly owned subsidiary of Honeywell International Inc., for the U.S. Department of Energy's National Nuclear Security Administration under contract DE-NA0003525.

SUMMARY

This report provides an analysis of the clad barrier function associated with the direct disposal of dual purpose canisters (DPCs) under hypothetical conditions in a shale repository and in an alluvial repository, including the effect of a postulated criticality event inside a disposed DPC. Should a postulated criticality event occur in a hypothetical shale repository, cladding will primarily degrade by general corrosion. Stress corrosion cracking, hydride cracking, creep failure, pitting and crevice corrosion, rod pressurization, and clad unzipping are calculated to have little impact on cladding persistence. At the higher temperature expected during a postulated criticality event in a saturated shale repository, general corrosion of cladding would be rapid - on the order of 0.034 microns/yr. A few hundred years after onset of a postulated criticality event in a shale repository complete general corrosion of fuel assembly grid spacer walls and guide tubes will likely result in settling of fuel rods upon each other. This rod consolidation should displace the water moderator and possibly terminate a postulated criticality. The primary potential degradation pathway for cladding in a hypothetical alluvial repository is localized corrosion by fluoride, which cannot occur in a shale repository. Fluoride-enhanced corrosion of cladding would be accelerated under the slightly higher (< 100°C) temperatures associated with a postulated criticality event. The impact of criticality in both cases (shale and alluvial) would be to increase the amount of failed cladding. But it would require very specialized transport pathways.

ACKNOWLEDGEMENTS

This work was supported by the DOE Office of Nuclear Energy, through the Office of Spent Fuel and Waste Science and Technology. We greatly appreciate the technical review of Rob Howard.

CONTENTS

SUMMARY iii

ACRONYMS 9

1. INTRODUCTION 11

2. CLADDING DEGRADATION 13
   - 2.1 Degradation of Cladding from Waterlogged Rods 13
   - 2.2 Degradation of Cladding Prior to Disposal 13
   - 2.3 General Corrosion 14
   - 2.4 Microbially Induced Corrosion of Cladding 15
   - 2.5 Localized (Radiation-enhanced) Corrosion of Cladding 16
   - 2.6 Localized (Pitting) Corrosion of Cladding 16
   - 2.7 Localized (Crevice) Corrosion of Cladding 16
   - 2.8 Enhanced Corrosion of Cladding from Dissolved Silica 16
   - 2.9 Creep Rupture of Cladding 16
   - 2.10 Internal Pressurization of Cladding 18
   - 2.11 Stress Corrosion Cracking of Cladding 20
   - 2.12 Hydride Cracking of Cladding 20
   - 2.13 Cladding Unzipping 21
   - 2.14 Mechanical Impact on Cladding 22
   - 2.15 Diffusion-controlled Cavity Growth in Cladding 22
   - 2.16 Localized (Fluoride enhanced) Corrosion of Zircaloy 22

3. CONCEPTUAL MODEL FOR CLAD DEGRADATION WITH AND WITHOUT CRITICALITY FOR LATE WP BREACH 25

4. REFERENCES 27

LIST OF FIGURES

Figure 1. Oxide layer thickness as a function of burnup for ZIRLO® and Optimized ZIRLO™ (left, Pan et al. 2013) and M5® cladding (right, Mardon et al. 2010). 12

Figure 2. Fuel failure rates trending downward (EPRI 2008). 14

Figure 3. End-of-life rod internal pressure data extrapolated to 25°C (Billone and Burtseva 2020). 19

LIST OF TABLES

Table 1. Cladding-related FEPs. 13
Table 2. Fuel Failure Sources (Cohen 1999) 13
Table 3. Low temperature, near neutral pH Zirconium Degradation rates in the presence of Fluoride..... 22
Table 4. As-received Clad Degradation Mechanisms, Base Case and with Criticality. 25
Table 5. Zircaloy Thicknesses and 250°C Failure Times. 25

This page is intentionally left blank.

ACRONYMS

BWR	boiling water reactor
DCCG	diffusion-controlled cavity growth
DHC	delayed hydride cracking
FCRD	Fuel Cycle Research and Development
FEP	feature, event, and process
FMDM	fuel matrix degradation model
IAEA	International Atomic Energy Agency
kgU	kilogram uranium
MPa	Mega Pascal
MWd	Megawatt day
NFST	Nuclear Fuels Storage and Transportation Planning Project
PWR	pressurized water reactor
SCC	stress corrosion cracking
STP	standard temperature and pressure
WP	waste package

This page is intentionally left blank.

CLADDING DEGRADATION CONCEPTUAL MODEL

1. INTRODUCTION

Cladding integrity must be reliably estimated, or bounded, in repository licensing efforts because radionuclide release from breached waste packages (WPs) may be directly proportional to the fraction of cladding that is failed. Presently all repository programs make bounding assumptions of cladding's barrier performance. Finland's planned repository at Onkalo assumes that water will penetrate the canister insert and fuel cladding in 1000 years upon canister breach in their baseline scenario. In the safety analysis for Sweden's proposed repository at Forsmark "cladding is not assumed to constitute a barrier to radionuclide release from the fuel" (SKB (Svensk Kärnbränslehantering AB) 2011). The Canadian repository effort takes no credit for cladding. The Yucca Mountain Repository license application ultimately took no credit for cladding, that is all fuel rods were conservatively assumed to be directly exposed to in-package fluids upon WP breach and water entry. Although early analyses concluded that cladding at Yucca Mountain would limit radionuclide releases (e.g. Siegmann 2000), the overall calculated margin of safety was sufficient that the additional barrier function provided by cladding could be conservatively neglected.

As part of the consideration of new, generic repository designs, this report provides a reanalysis of the clad barrier function for hypothetical conditions associated with the direct disposal of dual purpose canisters (DPCs). One aspect that was not previously considered, but that is being analyzed going forward is the effect of a postulated criticality event inside a disposed DPC on clad barrier function. The present analysis reviews the cladding barrier function starting with the earlier analyses done for Yucca Mountain (Bale 2000, Siegmann 2000, Siegmann 2000, Macheret 2001, Siegmann 2004), and recent work of Hardin et al. (2019). New outputs are: 1. An updated analysis of the impacts of localized corrosion due to evaporative concentration of salts, 2. An analysis of high temperature creep during a postulated shale criticality, 3. Calculation of postulated criticality impacts on internal rod pressure, and 4. A closer examination of Zircaloy cladding and spacer grid degradation during a postulated criticality.

Upon disposal, the only failed Zircaloy cladding will be the cladding that failed in the reactor, or during transportation and disposal operations. Zircaloy is typically coated by a durable, rapidly self-healing passivation layer of ZrO_2 that makes it resistant to most groundwaters and in-package fluids, as well as microbial attack, in a repository. Repository time-scale evolution of Zircaloy must account for potential degradation by stress corrosion cracking (SCC), delayed hydride cracking (DHC), pitting, and creep. More cladding may fail if a DPC-based WP experiences a criticality event and reaches higher disposal temperatures where Zircaloy degrades much more rapidly, particularly through general corrosion. Degradation rates of Zircaloy grid spacers and guide tubes are of particular interest since they are thin, and their degradation might allow fuel rod consolidation and criticality termination. Hardin et al. (2019) noted "oxidation and localized corrosion are most appropriate for consideration in response to disposal criticality, because of elevated temperature and the potential for evaporative concentration of solutes during repeated, episodic heating events."

A postulated criticality event in a repository sited in unsaturated alluvium will result in peak temperatures that do not exceed 100ºC; whereas criticality could cause temperatures in a saturated shale repository to reach 250ºC. Note that these temperatures are still significantly below the typical cladding temperatures of approximately 275°C - 315°C in a Pressurized Water Reactor (PWR) and a maximum of approximately 285°C in a Boiling Water Reactor (BWR). Note that the focus here is on cladding degradation upon WP breach after the packages have cooled. Future analyses should consider cladding degradation under the higher temperature conditions of early WP breach. Fluoride salts, able to damage cladding, might be concentrated in the alluvial repository; no such concentration could happen in the shale repository. In-package fluids in both repositories would be near neutral, before and during a postulated criticality event (Price, Alsaed et al. 2020). The shale fluids would be more reducing (higher H_2 pressures), particularly at the high temperatures of a postulated criticality event because of the accelerated degradation of steel.

The analysis below focuses on PWR cladding, as opposed to BWR cladding because BWR cladding is thicker than PWR cladding, 813 vs 570 microns, has lower burnup, and experiences less hoop stress due to a significantly lower initial helium rod backfill pressure. However, the evolution in BWR assembly design from a typical 8×8 assembly to the now prevalent 10×10 assembly design and now the introduction of 11×11 designs is resulting in the cladding dimensions and especially the cladding thickness of BWR rods approaching those of PWR rods. Whereas the rod internal pressures for BWR cladding is much lower, BWR cladding tends to corrode more than PWR cladding because of the aggressive nature of steam. For the purpose of this analysis, we will assume that BWR cladding performance is bounded by PWR cladding; however, for a few mechanisms such as general corrosion, that may not be the case and should be investigated as warranted for repository performance.

Zircaloy 2 was and is still used for BWR cladding. Zircaloy 4 was the primary alloy used for PWR cladding until the late 1990s and early 2000s. Zircaloy 4 contains less nickel and more iron than Zircaloy 2. With the push to achieve higher burnups, the industry developed zirconium-based alloys that are more resistant to oxidation and hydrogen pickup, two of the main factors that limit the burnup for Zircaloy-4 clad fuel. Framatome introduced M5® cladding, a fully-recrystallized zirconium-niobium alloy with no tin and controlled oxygen, iron and sulfur content in the mid-1990s. Westinghouse introduced ZIRLO®, which is also stress-relief annealed zirconium-niobium alloy but still contains some tin. By 2010, full core loads of Optimized ZIRLO™, which is partially-recrystallized and has optimized tin content, have been in use for PWRs. All these newer alloys have significantly less oxidation and hydrogen pickup during irradiation in a reactor (see Figure 1) and have superior creep and growth performance relative to Zircaloy-4. For this report, the effects of newer cladding alloys will be ignored. Only 1 – 2% of the fuel slated for Yucca Mountain was to be stainless steel, not Zircaloy. Stainless steel clad was assumed to be failed before disposal and provide no barrier function at Yucca Mountain.

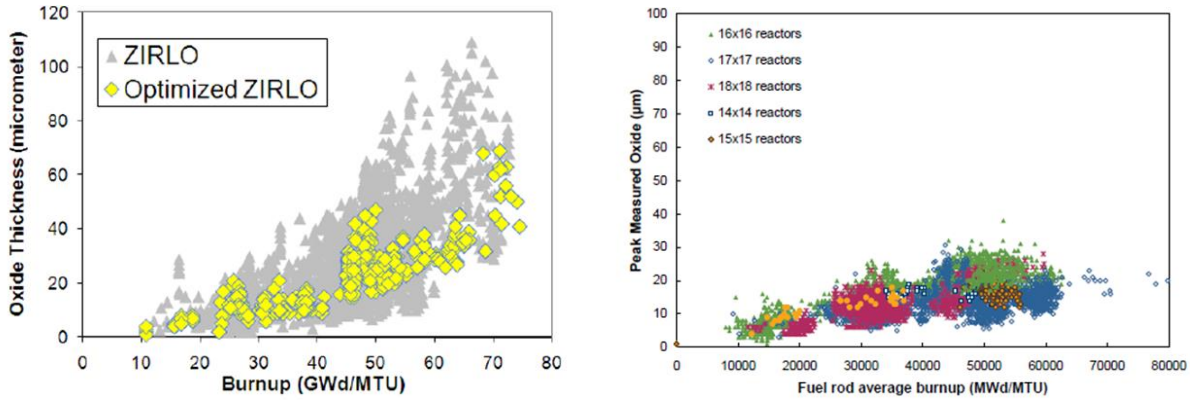

Figure 1. Oxide layer thickness as a function of burnup for ZIRLO® and Optimized ZIRLO™ (left, Pan et al. 2013) and M5® cladding (right, Mardon et al. 2010).

The initial state of the cladding and fuel burnup are important indicators of long-term stability. As-received cladding that has failed is more likely to unzip. Fuel burnup affects the amount of surface oxidation, absorbed hydrogen, fission gas production and release, increased internal rod pressure, and fuel pellet swelling and the corresponding free volume reduction (Siegmann 2000).

2. CLADDING DEGRADATION

The Features, Events, and Processes (FEPs) associated with cladding degradation at Yucca Mountain (Table 1) identify the primary potential cladding degradation modes. All have been observed experimentally (except 2.1.02.18.0A), but not all will be important under repository conditions. Some will not be affected by a postulated criticality event because they occur before disposal – degradation of cladding from waterlogged rods and degradation prior to disposal - but are briefly reviewed below anyway.

Table 1. Cladding-related FEPs.

2.1.02.11.0A	Degradation of cladding from waterlogged rods
2.1.02.12.0A	Degradation of cladding prior to disposal
2.1.02.13.0A	General corrosion of cladding
2.1.02.14.0A	Microbially influenced corrosion of cladding
2.1.02.15.0A	Localized (radiolysis enhanced) corrosion of cladding
2.1.02.16.0A	Localized (pitting) corrosion of cladding
2.1.02.17.0A	Localized (crevice) corrosion of cladding
2.1.02.18.0A	Enhanced corrosion of cladding from dissolved silica
2.1.02.19.0A	Creep rupture of cladding
2.1.02.20.0A	Internal pressurization of cladding
2.1.02.21.0A	Stress corrosion cracking of cladding
2.1.02.22.0A	Hydride cracking of cladding
2.1.02.23.0A	Cladding unzipping
2.1.02.24.0A	Mechanical impact on cladding
2.1.02.26.0A	Diffusion-controlled cavity growth in cladding
2.1.02.27.0A	Localized (fluoride enhanced) corrosion of cladding

2.1 Degradation of Cladding from Waterlogged Rods

Siegmann (2000) discounted any effect of spent pool storage on cladding condition citing reviews by the IAEA (1988) and DOE (Johnson 1977), concluding that "fuel failure or degradation is not expected during pool storage, and the fuel failure rates observed from reactor operation are appropriate for the cladding degradation analysis." Spent fuel pools typically maintain temperatures between 25°C and 35°C and are required to maintain temperatures ≤60°C and water purity is maintained; hence the very low degradation rates in U.S. spent fuel pools.

2.2 Degradation of Cladding Prior to Disposal

Siegmann (2000) calculated the as received failure rate of rods at Yucca Mountain to be 0.0155 – 1.285% (Median = 0.0948%). This represents failure due to reactor operations + pool storage + dry storage + handling/consolidation + transport. A broadly parallel analysis done by S. Cohen and Associates (1999) corroborated the results of Siegmann (2000) with a similar clad failure distribution, 0.01 – 1% (Stahl 2005); a median failure rate of 0.1% was chosen by Stahl (2005). Table 2 below separates out the individual origins of early clad failure.

Table 2. Fuel Failure Sources (Cohen 1999)

Fuel Service Period	Rod Failure %
In-Service	< 0.05
Pool Storage	0
Dry Storage	0.03
Consolidation	0.005
Other Handling	0.0003
Total	< 0.1

Reactor operations and dry storage cause the bulk of cladding damage, though the total amount is small. It was initially thought that creep would occur at the high temperatures of dry storage. The US Nuclear Regulatory Commission (NRC) recently (NRC 2019) found that while thermal creep during the first 60 years of dry storage is credible, "..due to the high creep capacity of zirconium-based alloys, thermal creep is not expected to result in cladding failures and reconfiguration of the fuel." Similarly, they conclude that "the low temperature (athermal) creep mechanism is not considered credible, even for the unlikely scenario where fuel reaches room temperature during the 60-year timeframe." Siegmann (2000) estimated dry storage to cause 0.045% of failures, and transportation to cause 0.01% of failures. Figure 2 shows the trend in fuel failures in the US between 1980 and 2007 (EPRI 2008). In 2006, the Institute of Nuclear Power Operations (INPO) set a goal to achieve zero fuel failures by 2010. While this goal has not yet been achieved, the failure rate continues to decrease. Recent multi-lab testing of three 17x17 PWR surrogate assemblies shipped from dry storage sequentially by truck, local ship, ocean-going ship, and rail from Spain to the center of the US confirm the small effect of transportation on fuel. The accumulated damage fraction in all cases was below 1E-10. The maximum strain observed during the tests resulted in stresses that were far below cladding yield limits (Kalinina, Ammerman et al. 2019). Thus, the failure rates of Siegmann (2000) and Cohen (1999) should be considered as an upper bound with fewer failures with more modern fuels.

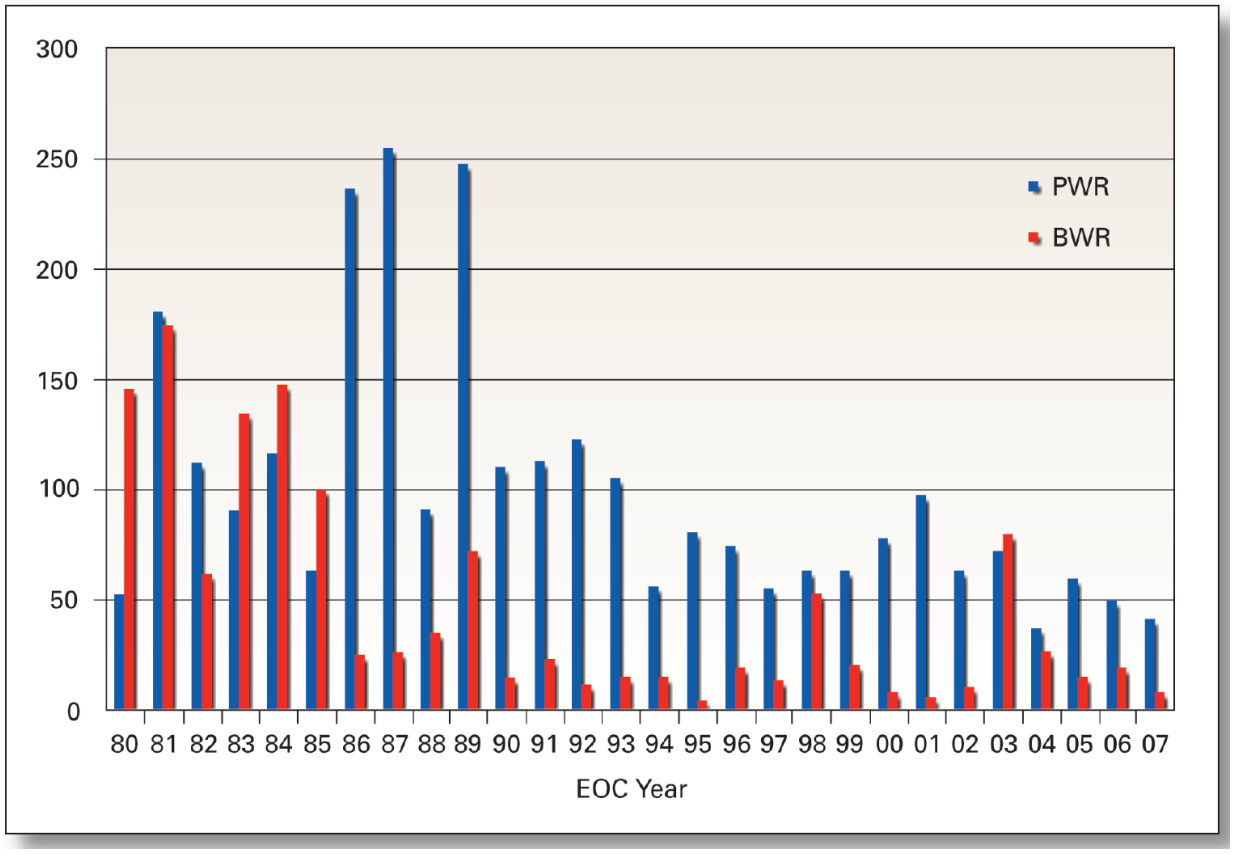

Figure 2. Fuel failure rates trending downward (EPRI 2008).

2.3 General Corrosion

General corrosion (oxidation) of Zircaloy is:

$$Zr + 2H_2O \rightarrow ZrO_2 + 2H_2 \quad [1]$$

and proceeds in 3 steps: 1. An early [high rate] pre-transition regime wherein the surface film grows by a cubic rate law, 2. A transition stage, and 3. A linear post-transition kinetic regime which is most relevant to a repository (Hillner, Franklin et al. 1998). Oxygen diffusion through the passivating ZrO_2 surface layer is believed to be the rate-limiting step (Hillner, Franklin et al. 1998).

The kinetics of the post-transition reaction was originally described by the rate expression (Hillner 1977):

$$\Delta W = 1.12 \text{ X } 10^8 \exp[-12{,}529/T] \text{ x } t \quad [2]$$

Where: ΔW is ZrO_2 weight gain (mg/dm^2), T is absolute temperature (^oK), and t is exposure time (days). Subsequent work (Hillner, Franklin et al. 1998) indicates that post-transition corrosion accelerates after a certain point, hence corrosion is described by two linear rate laws, the second repository-relevant rate law being:

$$\Delta W = 3.47 \text{ X } 10^7 \exp[-11{,}452/T] \text{ x } t \quad [3]$$

Equation 3 has been used to predict Zircaloy corrosion in a repository setting (Hillner, Franklin et al. 1998). Equation 3 predicts Zircaloy corrosion rates at 50^{o}C to be 2e-7 microns/yr; and 0.17 microns/yr at 250^{o}C (critical conditions). The rates used to build the general corrosion rate law of Hillner, Franklin, et al. (1998) were generally measured in near neutral solutions. They are applicable to the in-package environment because in-package pH's tend to remain near neutral as well (Price, Alsaed et al. 2020). General corrosion is relatively rapid under critical conditions because the sensitivity of general clad corrosion to temperature is so high (e.g. Siegmann 2004).

Irradiated Zircaloy degrades 2 – 20 times faster than non-irradiated Zircaloy (e.g. Figure 8.6 of IAEA (International Atomic Energy Agency) 1998) driven by radiation damage to both the passive surface layer and the underlying metal (Hillner, Franklin et al. 1998). Equation 3 is based on out-of-reactor autoclave experiments, and must be multiplied by at least a factor of 2 (Hillner, Franklin et al. 1998) to describe Zircaloy corrosion in a repository undergoing a postulated criticality event. There is considerable uncertainty in the underlying mechanism(s) of irradiation-induced acceleration of clad degradation (Section 9.2 of IAEA (International Atomic Energy Agency) 1998). Of relevance to saturated repositories is the observation that high hydrogen levels appear to greatly reduce the irradiation effect (Pg. 223 of IAEA (International Atomic Energy Agency) 1998). Annealing of rate-accelerating irradiation damage also occurs, particularly at high temperatures. Hillner et al. (1998) noted that clad degradation rates might be higher in a repository than autoclave-measured rates (and Equation 3) because of irradiation in the reactor before disposal, and conservatively assumed a factor of 2 irradiation acceleration, though noting the effect would probably be less. When considering criticality impacts on cladding below, the irradiation multiplier of 2 (Hillner, Franklin et al. 1998) is used with somewhat less conservatism because a postulated criticality event itself might cause irradiation damage to the clad.

Similar work on oxidation rates under repository conditions of the newer cladding alloys (M5®, ZIRLO®, and Optimized ZIRLO™) and of the new accident tolerant designs that have a thin coating of chromium on the outer diameter of the cladding has not been performed. However, given their resistance to oxidation under the high temperatures experienced in reactor operations (as in Figure 1), it is expected that oxidation under repository conditions would be significantly less than for Zircaloy-4.

2.4 Microbially Induced Corrosion of Cladding

Microbially induced corrosion of cladding is unlikely because Zircaloy is notably resistant to acid attack, particularly weak acids such as those produced by microbes (Hillner, Franklin et al. 1998). Zircaloy is unaffected by sulfate-reducing bacteria (McNeil and Odom 1994). Microbiologically induced corrosion, crevice corrosion, and pitting have not been observed in reactor operation or pool storage (Siegmann 2000). If anything, the high temperatures of a postulated criticality event would tend to inhibit microbial activity. Otherwise, no criticality effect is expected.

2.5 Localized (Radiation-enhanced) Corrosion of Cladding

Radiolytic production of nitric acid (alluvial case) and hydrogen peroxide (alluvial and shale) is unlikely to accelerate cladding corrosion in a repository environment because zirconium is inert in hydrogen peroxide (Yau and Webster 1987) and in up to 65% nitric acid (Siegmann 2004). pH shifts from nitric acid production in the alluvial case will be prevented by pH-buffering dissolution of corrosion products (Price, Alsaed et al. 2020). Radiation-enhancement of general corrosion by a postulated criticality event was analyzed above.

2.6 Localized (Pitting) Corrosion of Cladding

Clad pitting requires: low pH (pH < 2.5), sufficiently oxidizing ions – most notably Fe^{3+}; high concentrations of halides – particularly chloride > 1mM; and the presence of electrochemically conducive surface contaminants (e.g. Fahey, Holmes et al. 1997) or absence of the passivating oxide surface layer (Siegmann 2004). In-package fluids in a shale or alluvial repository would be near neutral pH, before and during a postulated criticality event (Price, Alsaed et al. 2020) even after being evaporatively concentrated (alluvial case). Growth of ferric (hydr)oxide minerals such as hematite or goethite will limit Fe^{3+} to sub-ppm levels under the oxidizing conditions of the alluvial repository; reduction of Fe^{3+} to Fe^{2+} will limit Fe^{3+} to sub-ppm levels in the shale repository. For comparison, Bale (2000) suggested that at least 50 ppm Fe^{3+} is needed to accelerate Zircaloy corrosion. The presence of non-conductive thick oxide layers on cladding should mitigate against pitting by electrochemically conducive surface contaminants, as would pickling (Bale 2000). In short, the enabling conditions for pitting will not exist for pitting corrosion in a repository, though the oxide thickness of newer alloys may make them more susceptible, nor would a postulated criticality event alter this absence of enabling conditions.

2.7 Localized (Crevice) Corrosion of Cladding

All evidence says Zircaloy will not corrode in a repository through crevice corrosion (e.g. Yau and Webster 1987, Fraker 1989, Siegmann 2004). Notes Bale (2000) “Zirconium is one of the most crevice corrosion resistant materials. For example, it is not subject to crevice corrosion even under such adverse conditions as low-pH chloride solutions or wet chlorine gas.” No effect of a postulated criticality event is expected to change this.

2.8 Enhanced Corrosion of Cladding from Dissolved Silica

There is no evidence for silica enhancing corrosion of cladding, but some indirect evidence (Siegmann 2004) that silica has no effect on cladding corrosion. No effect of a postulated criticality event is expected to change this.

2.9 Creep Rupture of Cladding

Creep rupture of cladding is more of a concern during dry storage and in the first several hundred years after disposal than long-term in a repository because of the higher temperatures involved. Unirradiated Zircaloy may sustain >10% strain without rupture, while high burnup fuel may fail at 4% strain (Hardin 2019). Tensile stress magnitude in the Zircaloy (hoop stress) of less than 90 MPa has been shown to substantially reduce the rate of creep strain accumulation (Hardin 2019). Internal pressurization of rods by gas production causes tensile stresses leading to creep, but only at relatively high temperatures > 300°C. Repository temperatures will be too low for creep rupture of cladding (Siegmann 2004), even should criticality occur and raise temperatures. Creep rupture was thought to be a significant degradation mechanism during dry storage where temperatures are higher, but recent work (NRC 2019, EPRI 2020) has shown that hoop stresses are significantly lower than originally hypothesized and thermal creep is not expected to result in cladding failures and reconfiguration of the fuel during dry storage. Unlike most other cladding failure mechanisms, creep rupture does not require waste package breach and contact with fluids. Key to creep rupture is the gas pressure internal to the rod which is a function of the amount of gas and the

available void volume. To the gas initially present in the rod are added fission product gasses which depend upon fuel burnup and power in the reactor (see Section 2.10). The internal void volume is made up of fuel-cladding gaps, pellet-pellet gaps and plenum volume (e.g. Hardin 2019). Also, the fuel pellets swell slightly with burnup.

Independent of increased gas pressure, cladding creep is sensitive to thinning due to corrosion (oxide layer formation) and cladding embrittlement. Cladding that has been thinned or embrittled will rupture at lower total creep strains. Cladding creep may result in rupture if the total creep strain exceeds a threshold of about 6%. Unirradiated Zircaloy may sustain >10% strain without rupture, while high burnup fuel may fail at 4% strain (Hardin 2019). Irradiation embrittlement causes creep rupture where burnup is greatest – near the center of the rod.

Cladding creep failure was estimated for Yucca Mountain (Siegmann 2000) by comparing predicted strain, using Murty correlations measured between cladding temperature history and observed creep strain, against probabilistic estimates of the critical strain needed for cladding failure. Murty correlations sum together expressions that account for high stress glide creep and low stress Coble creep (Henningson, Willse et al. 1998) in unirradiated cladding at a specific time, t (hours). Murty correlations were chosen over Matsuo correlations because they specifically consider Coble creep, a mechanism likely to be observed in the relatively low temperatures of a repository. ε is dimensionless and must be multiplied by 100 to calculate % creep:

$$\varepsilon = \varepsilon_{glide} + \varepsilon_{glide}$$

$$\varepsilon_{glide} = \dot{\varepsilon}_{glide} t + \frac{K \varepsilon_T \dot{\varepsilon}_{glide} t}{\varepsilon_T + K t \dot{\varepsilon}_{glide}}$$

$$\dot{\varepsilon}_{glide} = 4.97\ x\ 10^6 e^{-31200/T} \frac{E}{T} [\sinh\left(807 \frac{\sigma}{E}\right)]^3$$

$$\varepsilon_{Coble} = 8.83 e^{-2100/T} \frac{\sigma}{T} t$$

Where $\varepsilon_T = 0.008, K = 10, E = (1.148\ x\ 10^5 - 59.9T) x\ 10^6, T =$ Temperature (Kelvin), and $\sigma =$ stress (Pa).

The Murty equations above were modified to account for lower clad creep that is observed by irradiated clad at high temperatures with the following equation (CRWMS M&O 2000):

$$\mathrm{MM}(\%) = 0.233 * \mathrm{M}(\%)^{0.488}$$

Where M is the % creep strain predicted by the unmodified Murty equations above for unirradiated clad and MM is the % creep strain predicted for irradiated clad.

Accumulated creep at time t_i is calculated with the following equation over assumed clad temperature-time segments (Siegmann 2000).

$$\varepsilon(t_i) = \varepsilon(T_{i-1}, t_{i-1}) + [\varepsilon(T_i, t_i) - \varepsilon(T_i, t_{i-1})]$$

A conservative creep-failure relationship was approximated by Siegmann (2000) from irradiated cladding failure tests as:

Fs = 14.4 – 135P; $0.0 < P \leq 0.06$

Fs = 6.77 – 7.81P; $0.06 \leq P \leq 0.5$

Fs = 5.33 – 4.93P; $0.5 < P < 1.0$

Where Fs is the strain failure limit (%) and P is a random probability between 0 and 1.

The approach of Siegmann (2000) when applied to the higher temperature of a hypothetical shale repository undergoing a postulated criticality event estimates an additional 0.191% creep strain, at 250°C for 10,000 years for cladding under a [relatively high] stress of 100 MPa. 0.191% additional creep is very small compared to the failure probability relations noted above, suggesting that a postulated criticality event will have little tangible impact on creep failure of cladding in a shale repository. The additional creep strain caused by a much lower temperature (< 100°C) postulated criticality event in a hypothetical alluvial repository is orders of magnitude less than for shale, hence negligible.

2.10 Internal Pressurization of Cladding

A relatively high internal rod pressure favors failure from cladding creep, hydride reorientation, DHC, and SCC (Siegmann 2000). Rod pressurization sets the cladding hoop stress and is a function of the available volume, temperature, the initial helium fill pressure (assumed for Yucca Mountain to be uniformly distributed between 2 and 3.5 MPa), and the production rates of gas phase fission products, primarily isotopes of Xe and Kr, fission gas release from the fuel matrix, and helium production from alpha decay. Once rods are removed from the reactor, fission product accumulation is sharply limited, but helium will continue to accumulate.

Siegmann (2000) developed a numerical expression for internal rod pressure over time by first building correlations between: fuel burnup and fission product release; temperature, time, and helium pressure; and burnup and fuel rod volume change. Siegmann (2000) calculated a mean internal rod pressure of 5 MPa at 100 years, 27°C, for a fuel burnup of 50 MWd/kgU; for a fuel burnup of 75 MWd/kgU the calculated internal pressure was 10 MPa. Siegmann (2000) set the rod plenum failure pressure to be the reactor system pressure, ~15 MPa at 320°C and ~7.5 MPa at 27°C. A 250°C failure pressure of 13 MPa is used below for the shale postulated criticality condition. Siegmann (2000) estimated that ~ 4.5% of the fuel rods going to Yucca Mountain approached the reactor system pressure. Figure 3 shows the room temperature end of life rod internal pressure at room temperature from the international, publicly available database, including work recently performed on the high burnup sibling pins at both Oak Ridge National Laboratory and Pacific Northwest National Laboratory. In the US, the NRC currently limits the peak rod-average burnup to 62 MWd/kgU. Note that the mean for burnups below the US limit of 62 MWd/kgU is approximately 4 MPa, which results in a pressure of only 9 MPa for a uniform temperature of 400°C. One of the major reasons that rod internal pressures, and thus hoop stresses, are significantly lower than previously estimated is that the initial fill pressure of helium has been decreasing in newer designs.

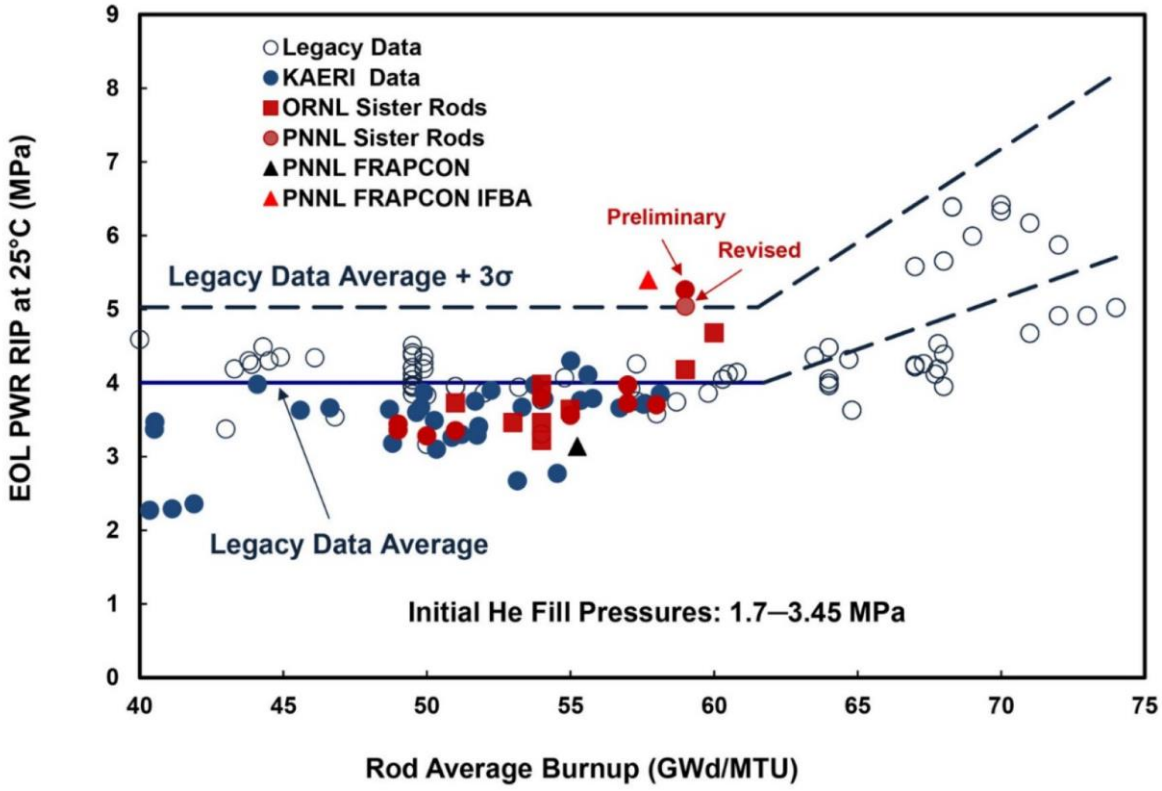

Figure 3. End-of-life rod internal pressure data extrapolated to 25°C (Billone and Burtseva 2020).

Fission gas production is linearly proportional to the fuel burnup, 31 cm^3 (STP)/MWd. Decay of fission product gases over the lifetime of a repository will be small (pg. 25 of Siegmann 2000) as most are stable (except for ^{85}Kr with a 10 year half life). Most of the fission gases are not released, but remain in the fuel matrix. Fission product release from the matrix depends upon burnup but mostly the power history of the fuel (Siegmann 2000). A postulated criticality event would cause a resurgence in fission product accumulation, and would probably minimally increase their release from the fuel matrix because of increased fission product diffusion at high temperatures (shale case). The reason is that during reactor operations with very high power relative to the post-closure postulated criticality scenarios, the fuel pellet centerline temperatures range between 800°C and 1200°C with fuel pellet surface temperatures close to that of the cladding and coolant, ~300°C. It is this large temperature gradient, especially in high burnup fuels, that drives the small amount of fission gas release. An EPRI study (EPRI 2013) found that "the weak dependence of the number of moles exhibited in Figure 3-7 may be indicative of the fact that the contribution of moles from fission gas release is small compared to the initial fill gas for the general population of fuel rods."

The much lower powers during a post-closure postulated criticality event will have a negligible effect on fission gas release and rod pressurization. For example, a steady-state criticality at a power level of 4 kW for 10,000 years would result in an additional ~1 MWd/kgU average burnup in a typical DPC. A steady-state criticality at a power level of 400 W lasting 10,000 years would result in an additional ~0.1 MWd/kgU average burnup in a typical DPC (Price, Alsaed et al. 2020). The added burnup from these postulated criticality events is less than 1% of the average burnup assumed for Yucca Mountain fuel (~ 45 MWd/kgU), hence would result in an insignificant increase in fission gas pressure. Calculations done by Oak Ridge [K. Bannerjee] for a 2.1 kW criticality event for 15,000 years indicate a minor (< 1%) increase in fission product Kr and Xe gasses from the baseline, non-critical case. The criticality temperature shift from 50 to 250°C (shale case) alone would increase the rod pressure by ~ 60%, a much larger increase.

Johnson and Gilbert (1983) calculated He pressure buildup from alpha decay for a fuel with 36 MWd/kgU burnup showing that it would become a significant contributor (Helium Pressure > 1 MPa) to total internal rod pressure in a repository after ~ 1000 years. Independently of time, the calculated He pressure becomes greater at higher temperature as well. Again, a criticality-driven jump in temperature alone from 50 to 250°C would amount to a 60% increase in internal rod pressure. In short, the primary effect of a postulated criticality event will be to increase rod pressure by raising temperature. However, as demonstrated in Figure 3, even assuming the average +3σ value of 5 MPa at 25°C, the pressure at 250°C would still only be < 9 MPa.

2.11 Stress Corrosion Cracking of Cladding

Stress corrosion cracking occurs by cracks propagating in materials subjected to a combination of concentrated local stress and aggressive chemicals concentrating at crack tips (Fraker 1989, Siegmann 2000). Initially for Yucca Mountain, any rod with a hoop stress calculated to be greater than 180 MPa (twice the cladding creep threshold of 90 MPa) was assumed to fail from SCC (Siegmann 2000) based on the results of Tasooji et al. (1984) (Pescatore et al. (1990) argued for an even higher SCC clad stress threshold of 200 MPa; and NRC (2019) states "…analysis indicates that at least 240 MPa of hoop stresses are needed to induce SCC for both Zircaloy-2 and Zircaloy-4). Siegmann (2000) calculated hoop stress from predicted internal pressures (see above), clad thinning by corrosion, and clad crack distribution. If the requisite stress existed, SCC could be driven by Cs and I (fuel-side SCC) or chloride (water-side SCC). Rapid repassivation tends to protect Zircaloy from stress corrosion cracking. Zirconium and its alloys are resistant to SCC in seawater, most aqueous environments and some sulfate and nitrate solutions (e.g. Fraker 1989).

Hardin et al. (2019) noted that "Hoop stress is less than 90 MPa for the great majority of spent fuel cladding even at elevated temperature up to 350°C, and virtually all cladding at lower temperatures". Because the stresses required for SCC "are higher than those expected to predominate in actual cladding, even at elevated temperature … SCC is unlikely if temperature is limited (as would be the case for criticality events in an unsaturated repository with maximum temperature limited by boiling) or there is a constant supply of diluent ground water (saturated repository)" (Hardin 2019).

2.12 Hydride Cracking of Cladding

During delayed hydride cracking hydrides slowly form at a crack tip causing the crack to propagate. DHC requires an incipient crack or defect from manufacturing or irradiation, hydride at the crack tip, and sufficient stress to propagate the crack (e.g. Siegmann 2004). Hydride is a separate Zr hydride phase or solid solution, and is formed by hydrogen existing as an impurity in the Zircaloy or produced from, for example, steel corrosion. Recall that although hydrogen will be particularly abundant under the reducing conditions of the shale repository scenario, hydrogen generated from corrosion of WP internals should not be able to penetrate the ZrO_2 surface layer on the cladding (Siegmann 2004). Zr hydride flakes are brittle and allow more rapid fracture propagation. Countering DHC is the general resilience of the Zircaloy oxide surface layer which will persist as long as water is available.

In theory, hydrogen transfer to cladding might also occur upon galvanic corrosion of basket steels in contact with Zircaloy. The process requires sustained intimate metal-metal contact with high contact pressures and is, even then, transient because corrosion breaks the metal-Zircaloy contact (Siegmann 2004). DHC was screened out at Yucca Mountain again [in part] because hydrogen was thought unlikely to penetrate the passive ZrO_2 surface coating of the cladding. Cladding stresses were also calculated to be too low for DHC to occur. Stress intensity factors are calculated to have a mean of 0.47 MPa-$m^{0.5}$ (range 0.002 to 2.7 MPa-$m^{0.5}$), which is below the threshold stress intensity factors that are in the range of 5 to 12 MPa-$m^{0.5}$ (Siegmann 2000, Siegmann 2004). The recent evaluation by EPRI (EPRI 2020) found that over a range of realistic hoop stresses, the critical crack size to sustain delayed hydride cracking are unrealistically large, often greater than the cladding wall thickness. Hydride reorientation, which facilitates crack propagation,

requires high thermal gradients and high stress, neither of which is expected in the repository environment (Siegmann 2004). Notes Hardin et al. (2019) "Delayed hydride cracking has been analyzed in terms of stress intensity and found to be unlikely even at elevated temperature, so that only a small fraction of fuel (0.01%) could be affected." A postulated criticality event is therefore expected to have no effect.

2.13 Cladding Unzipping

Clad unzipping occurs when oxidation of exposed fuel in contact with water causes an autocatalytic peeling of the clad because of formation of oxidized uranium phases having a higher volume than the fuel [UO_2] itself, e.g. $2H_2O + UO_2 + 1/2O_2 \rightarrow UO_3{:}2H_2O_{Schoepite}$; $\Delta Volume = V_{Schoepite} - V_{UO2} = 66.70 - 24.62 = 42.08$ cm^3. Unzipping does not occur when fuel dissolves non-oxidatively under completely reducing conditions [E_H < ~ 100 mV at pH 7 (Figure 1 Jerden, Frey et al. 2015)] because a higher volume alteration phase is not formed, e.g. $2H_2O + UO_2 \rightarrow U(OH)_4^{aq}$. Oxidative UO_2 dissolution is relatively rapid, 1 - 10 g/m^2day (Jerden, Thomas et al. 2020), though fuel degradation likely decreases sharply with burnup. Under completely reducing conditions, non-oxidative UO_2 dissolution is much slower, ~ 0.001 g/m^2day (Jerden, Thomas et al. 2020).

In between oxidizing and reducing conditions [E_H > ~ 100 mV at pH 7 (Figure 1 Jerden, Frey et al. 2015)}] where electron donors and acceptors are both present, is where fuel dissolution is most complex. The Fuel Matrix Degradation Model [FMDM] of Jerden and co-workers (e.g. Jerden, Frey et al. 2015, Jerden, Thomas et al. 2020) aims to predict fuel degradation rates under these conditions. FMDM is a mixed potential model that simultaneously accounts for alpha radiolysis and radiolytic production of oxidants as a function fuel burnup, accumulation of alteration phases at the spent fuel surface, H_2 production by corroding steels and Zircaloy, and electron transfer reactions occurring at/near the spent fuel surface and in the bulk solution (e.g. Jerden, Frey et al. 2015). A key feature of the FMDM is its ability to capture the inhibitory effect of dissolved H_2 on fuel degradation rates (e.g. Carbol and Spahiu 2005, Shoesmith 2013). Experimental validation of the FMDM is ongoing.

A postulated criticality event for the shale repository scenario should indirectly accelerate H_2 production from steel and Zircaloy corrosion because of the rise in temperature. Radiolytic production of H_2O_2 will be directly increased by the criticality itself, but so will production of radicals that react with H_2O_2. The difference between H_2 production and H_2O_2 production and reaction will determine whether oxidative fuel degradation, and unzipping, are inhibited. An alluvial repository might maintain the potential for unzipping because there would be renewed H_2O_2 production from radiolysis but less of a temperature-driven increase in H_2 production than in the higher temperature shale criticality.

Unzipping, should it occur, is a 2-step process: incubation at the site of fuel exposure, followed by splitting away from the fuel exposure site (Einziger and Strain 1986). Hardin et al. (2019) examined clad unzipping under a high temperature postulated criticality event event and noted that:

1. The time-to-splitting after perforation would be a few weeks at high temperature (283°C) but more than a million years at 100°C.

2. For splitting to occur at a rate significant to repository performance, elevated temperature >100°C is required.

Two end-member scenarios therefore exist for late WP breach:

1. In the oxidative alluvial repository with and without criticality, incubation and splitting would occur at rates so low as to never occur because temperatures would never exceed 100°C, and

2. In a highly reducing shale repository with or without criticality, splitting could not occur because of the absence of oxidative fuel dissolution.

Again, early WP breach might expose cladding to temperatures > 100°C. Temperatures might also exceed 100°C in individual rods that are uncovered in the alluvial scenario post-evaporation.

2.14 Mechanical Impact on Cladding

At Yucca Mountain, severe seismic events occurring at a frequency of 1.1 x 10^{-6}/yr were assumed to fail all the cladding (Siegmann 2000). Static loading from rockfalls was assumed to fail cladding beginning when open patches made up 50% of the WP surface, thereby allowing static loading of the rods.

2.15 Diffusion-controlled Cavity Growth in Cladding

Diffusion-Controlled Cavity Growth (DCCG) is the development of micro-cavities at high temperatures and stresses on grain boundaries causing the separation of the latter. The theory is that metallic materials subjected to high temperatures and stress might develop micro-cavities on grain boundaries, leading to decohesion of the metal grains. DCCG has been hypothesized but never observed in Zr-based cladding (Electric Power Research Institute 2020).

Lastly, nodular corrosion and crud-induced localized corrosion of Zircaloy requires copper (Fraker 1989) which will be absent in the WP. Nodular corrosion also requires T > 450ºC (IAEA (International Atomic Energy Agency) 1998), higher than would be achieved in a repository even if criticality occurred. Therefore a postulated criticality event will have no impact on DCGG.

2.16 Localized (Fluoride enhanced) Corrosion of Zircaloy

Fluoride can accelerate Zircaloy corrosion, but fluoride must be concentrated to higher levels by evaporation (e.g. Siegmann 2004). Evaporative concentration of fluoride can only occur in the alluvial repository where cyclic wetting and drying might occur, but not in a shale repository. Bale (2000) reviewed localized corrosion of Zircaloy, noting that fluoride accelerates general corrosion – especially at low pH; all other halides prompt pitting (see above). General corrosion of Zircaloy corrosion is accelerated by hydrofluoric acid, HF, the dissolved form of fluoride below pH ~ 3.2 at 25ºC; above pH 3.2 fluoride is present in solution primarily as fluoride ion, F^-, or alkali fluoride complexes, e.g. CaF^+. The fluoride effect on Zircaloy degradation is pronounced at low pH where most fluoride is present in the acid form, HF.

Table 3. Low temperature, near neutral pH Zirconium Degradation rates in the presence of Fluoride.

pH	Temperature (ºC)	Solution (mg/L)	HF activity	Corrosion rate (microns/yr)
5	55	5000 NaF	2.4e-6	8
5	55	1000 NaF + 4000 CaF_2	1.9e-6	6
6.5	55	1000 NaF	6.1e-8	6
7	100	[a]100 NaF	1.5e-6	8

All solutions were: 1.5% $CaCl_2$ + 1.5% NaCl + 1.0% $MgCl_2$ + 1.0% KCl except for the bottom one – which was "City Water" [assumed to be distilled water in the subsequent calculations]. [a]Approximately the same rate was measured when fluoride was added as sodium monofluorophosphate.

At the near neutral pH of the alluvial and shale repositories (Price, Alsaed et al. 2020), the fluoride effect will be sharply diminished because of the low activity of HF. Table 3 lists the near neutral pH Zircaloy degradation rates in the presence of fluoride cited in Bale (2000). The HF activities in Table 3 were calculated with PHREEQC (Parkhurst and Appelo 1999) assuming equilibrium precipitation of CaF_2 and MgF_2.

Bale (2000) concluded "If the pH is greater than 3.18 and the fluoride concentration is less than 5 ppm, then Hillner's equation can be used at any temperature". The general corrosion rate law of Hillner et al. (1998) would predict far lower HF-free 55 – 100ºC Zircaloy corrosion rates of 4e-7 to 2e-5 microns/yr than the HF-present rates in Table 3. The 5 to 7 order of magnitude difference in rate between HF-absent dissolution and dissolution in the presence of only micromolar activities of HF suggests either: 1. HF is extremely

effective at dissolving Zircaloy, 2. The rates cited in Bale (2000) measured the early, accelerated 'cubic' rates, and/or 3: Another HF-free general corrosion mechanism besides the one measured by Hillner et al. (1998) operates at low temperatures. Note that the Hillner et al. (1998) rate law is extensively calibrated but only at high temperatures, > 270°C. For comparison, Jerden et al. (2020) used an electrochemical technique [as opposed to weight gain measurements considered by Bale (2000)] to measure an HF-free, 25°C, pH 7, [NaCl] = 0.0043M Zircaloy corrosion rate of 0.19 g/m^2yr, which is equivalent to 0.03 microns/yr. Smith's (1988) electrochemical scoping experiments saw effectively no general corrosion (< 0.1 microns/yr) at 90°C in tuff-equilibrated J-13 water and stated that "The results suggest that the very slow oxidative corrosion predicted by extrapolation of higher temperature oxidation models to this lower temperature condition may be of the correct order of magnitude."

Sorting out if, and how, evaporatively concentrated waters might reach pH < 3.18 and fluoride levels might exceed 5 ppm is key to predicting accelerated cladding corrosion in the alluvial case (Hardin 2019). PHREEQC calculations of baseline (non-critical) reaction of Al and steels with alluvial groundwaters, and evaporation, at 50°C predict an in-package fluid of pH 7.6 < pH < 8.4. Fluoride levels reach approximately 100 ppm when the incoming water is evaporated fifty-fold. Corrosion products and secondary phases allowed to form upon equilibration in the calculation were again: NiO, Chromite, Hematite, Magnetite, Boehmite, Trevorite, Ni_3S_2, Quartz, Pyrite, Pyrhhotite, Chrysotile, Calcite, Brucite, and the fluoride minerals Fluorite and Sellaite. The P_{CO2} was set to $10^{-2.5}$ consistent with observed elevated soil and groundwater CO_2 levels. The partial pressure of oxygen was set to 10^{-20} atm to reflect the observed range of redox state of groundwaters, $0 < E_H < 300$ mV. The specific water composition used in the calculation was that of Ue5ST-1 115.0-115.25, taken from Estrella et al. (1993) and cited as an example of Great Basin alluvial waters by Mariner et al. (2018). Fluoride levels were set to 2.2 ppm, that of J-13 well water at Yucca Mountain. The geochemical calculations indicate that high fluoride concentrations are achievable through evaporative concentration; but low pH is not.

Hydrolytic production of nitric acid by a postulated criticality event was estimated (Price, Alsaed et al. 2020) to cause no significant change in in-package pH in the alluvial case from near neutral conditions primarily because of pH buffering by corrosion products inside the package. This means the maximal Zircaloy degradation rate in the alluvial case with a postulated criticality event will be approximately those in Table 3, 7 microns/yr. In the absence of criticality, the rates will be effectively zero, i.e. the much lower rate predicted by the Hillner et al. (1998) rate law.

This page is intentionally left blank.

3. CONCEPTUAL MODEL FOR CLAD DEGRADATION WITH AND WITHOUT CRITICALITY FOR LATE WP BREACH

The primary potential degradation pathway for cladding in a hypothetical alluvial repository will be local corrosion by fluoride. General corrosion is expected to be the primary degradation pathway in a shale repository undergoing a postulated criticality. Table 4 collects all as-received degradation mechanism (with the exception of Mechanical impact on cladding) and bins them as being unlikely (low probability), little effect or too slow (low consequence), or • (likely and high consequence).

Table 4. As-received Clad Degradation Mechanisms, Base Case and with Criticality.

	Alluvium		Shale	
Mechanism	**Base**	**Critical**	**Base**	**Critical**
General corrosion	too slow	too slow	too slow	•
Microbially influenced corrosion	unlikely	unlikely	unlikely	unlikely
Localized (radiolysis enhanced) corrosion	unlikely	unlikely	unlikely	unlikely
Localized (pitting) corrosion	unlikely	unlikely	unlikely	unlikely
Localized (crevice) corrosion	unlikely	unlikely	unlikely	unlikely
Enhanced corrosion from dissolved silica	unlikely	unlikely	unlikely	unlikely
Creep rupture	little/no effect	little/no effect	little/no effect	little/no effect
Internal pressurization of cladding	little/no effect	little/no effect	little/no effect	little/no effect
Stress corrosion cracking of cladding	unlikely	unlikely	unlikely	unlikely
Hydride cracking	unlikely	unlikely	unlikely	unlikely
Cladding unzipping	too slow	too slow	unlikely	unlikely
Diffusion-controlled cavity growth	unlikely	unlikely	unlikely	unlikely
Localized (fluoride-enhanced) corrosion	•	•	unlikely	unlikely

A postulated criticality event may have a high probability, high consequence impact on general corrosion in the shale case and fluoride-enhanced corrosion in the alluvial case, though more analysis is required. At the higher temperature expected for a postulated criticality event in a saturated shale repository general corrosion of cladding will be rapid - on the order of 0.34 microns/yr. Table 5 gives the time required for cladding, grid spacer walls, and guide tubes in a 17 x 17 PWR fuel rod array to dissolve completely by general corrosion at 250ºC (Price, Alsaed et al. 2020).

Table 5. Zircaloy Thicknesses and 250ºC Failure Times.

	Thickness (mils)	Failure time (years)
Cladding	[a]22.5	[b]1640
Grid spacer walls	[c]10	[d]366
Guide tubes	[e]16	[d]585

[a](Westinghouse Electric Company LLC 2011). [b]Outside-in corrosion only. [c](Fascitelli and Durbin 2020). [d]Corrosion from both sides.

The results in Table 5 indicate that a few hundred years after onset of shale repository criticality complete general corrosion of fuel assembly grid spacer walls and guide tubes will result in settling of fuel rods upon each other. This rod consolidation could exclude the water moderator and might terminate a postulated criticality (Alsaed, A, 2019, Permanent Criticality Termination Processes in Disposed DPCs, M4SF-

20SN010305063), though it will depend upon the final configuration of the rods. Not lastly that the Zircaloy failure times calculated above are maxima for overall failure; since "gross damage will ensue when the surface retreat reaches approximately half the thickness" (Hardin 2019).

Fluoride-enhanced corrosion of cladding can only occur in the alluvial repository. It would be accelerated under the slightly higher (< 100°C) temperatures of a postulated criticality event. The impact in both cases would be to increase the amount of failed cladding. But to do so would require very specialized transport pathways. The Yucca Mountain model for fluoride-enhanced cladding corrosion (Siegmann 2000), envisioned fluoride entering a breached waste package to completely degrade the cladding on a 10 mm reach (the width of a drip) of a single fuel rod before degradation began on another rod. This scenario requires that cladding corrosion by fluoride be as fast [or faster] than the supply of fluoride by incoming water, that all of the relatively low levels of fluoride in Yucca Mountain seepage, ~2 ppm, react with cladding; i.e. no fluoride flows through the waste package without reacting. It also required no fluoride diversion from the 10 mm water splat region. Siegmann (2000) noted that "the actual wetted width would be wider because the rough, porous products of corrosion on the surface of fuel rods would tend to wick water and promote wider flow paths", which means less cladding degradation. The only scenario that failed a significant number of rods was this flow-through case. Fluoride coming into a "bathtub scenario" would encounter all of the rods and ultimately fail none.

4. REFERENCES

Bale, M. (2000). Clad Degradation - Local Corrosion of Zirconium and Its Alloys under Repository Conditions, ANL-EBS-MD-00001 2 REV 00.

Billone, M.C. and T.A. Burtseva. (2020) Preliminary Destructive Examination Results for Sibling Pin Cladding. ANL-19/53 Rev 2. M3SF-20PN010201011, February 28, 2020.

Carbol, P. and K. Spahiu (2005). The effect of dissolved hydrogen on the dissolution of 233U doped UO2(s) high burn-up spent fuel and MOX fuel, Swedish Nuclear Fuel and Waste Management Co.

Cohen, S. (1999). Effectiveness of Fuel Rod Cladding as an Engineered Barrier in the Yucca Mountain Repository. Cohen & Associates, McLean, Virginia.

CRWMS M&O (2000). Creep Strain Values and Correlation for Irradiated Spent Nuclear Fuel. Input Transmittal PA-WP-00383.T. Las Vegas, NV.

Einziger, R. E. and R. V. Strain (1986). "Behavior of breached pressurized water reactor spent-fuel rods in an air atmosphere between 250 and 360 C." Nuclear Technology **75**(1): 82-95.

Electric Power Research Institute (2020). Phenomena Identification and Ranking Table (PIRT) Exercise for Used Fuel Cladding Performance. EPRI, Palo Alto, CA: 2020. 3002018439

Electric Power Research Institute (2013). *End-of-Life Rod Internal Pressures in Spent Pressurized Water Reactor Fuel.* EPRI, Palo Alto, CA: 2013. 3002001949.

Electric Power Research Institute (2008). Executive Summary of *The Path to Zero Defects: EPRI Fuel Reliability Guidelines.* *http://mydocs.epri.com/docs/CorporateDocuments/SectorPages/Portfolio/PDM/FRP%20Exec%20Sum1c.pdf*

Estrella, R., S. Tyler, J. Chapman and M. Miller (1993). Area 5 Site Characterization Project: Report of hydraulic property analysis through August 1993, Nevada Univ., Las Vegas, NV (United States). Desert Research Inst.

Fahey, J., D. Holmes and T.-L. Yau (1997). "Evaluation of localized corrosion of zirconium in acidic chloride solutions." Corrosion **53**(1): 54-61.

Fascitelli, D. and S. Durbin (2020). Fuel assembly dimensions. P. V. Brady.

Fraker, A. (1989). Corrosion Behavior of Zircaloy Spent Fuel Cladding in a Repository. Nat. Inst. Stds. Tech.(NISTIR)-89-4114.

Hardin, E., Ed. (2019). DPC Criticality Simulation Preliminary Phase: Fuel/Basket Degradation Models M3SF-19SN010305071.

Henningson, P., J. Willse, B. Cox, M. Bale, K. Murty and W. Pavinich (1998). Cladding Integrity Under Long Term Disposal. Framatome Technologies, Document. **51:** 1267509-1267500.

Hillner, E. (1977). Corrosion of zirconium-base alloys—an overview. Zirconium in the Nuclear Industry, ASTM International.

Hillner, E., D. Franklin and J. Smee (1998). The Corrosion of Zircaloy-Clad Fuel Assemblies in a Geologic Repository Environment. Bettis Atomic Power Laboratory Report WAPD.

IAEA (International Atomic Energy Agency) (1988). Survey of Experience with Dry Storage of Spent Nuclear Fuel and Update of Wet Storage Experience. Technical Report Series, No. 290. Vienna, Austria: International Atomic Energy Agency.

IAEA (International Atomic Energy Agency) (1998). 996, Waterside corrosion of zirconium alloys in nuclear power plants. International Atomic Energy Agency Technical Document. **996**.

Jerden, J., K. Frey and W. Ebert (2015). "A multiphase interfacial model for the dissolution of spent nuclear fuel." Journal of Nuclear Materials **462**: 135-146.

Jerden, J., S. Thomas, E. Lee, V. K. Gattu and W. Ebert (2020). Results from Fuel Matrix Degradation Model Parameterization Experiments and Model Development Activities, ANL/CFCT-20/15, Argonne National Laboratory.

Johnson, A. (1977). Behavior of Spent Nuclear Fuel in Water Pool Storage. BNWL-2256. Pacific Northwest Laboratory.

Johnson, A. and E. Gilbert (1983). Technical basis for storage of Zircaloy-clad spent fuel in inert gases, Pacific Northwest Lab., Richland, WA (United States).

Kalinina, E., D. Ammerman, C. Grey, M. Arviso, C. Wright, L. Lujan, S. Saltzstein, S. Ross, N. Klymshyn, B. Hanson, A. Alonso, I. Perez, R. Garmendia, G. Calatuyad and W. Choi (2019). International Multi-Modal Spent Nuclear Fuel Test Transportation Test: The Transportation Test Triathlon, SAND2019-1995C, Sandia National Laboratories.

Macheret, P. (2001). Creep strain correlation for irradiated cladding CAL-EBS-MD-000015 REV 00, Yucca Mountain Project, Las Vegas, Nevada.

Mardon JP, GL Garner, and PB Hoffmann, in: Proceedings of 2010 LWR Fuel Performance/TopFuel/WRFPM, Orlando, Florida, 26-29 September, p. 577. American Nuclear Society.

Mariner, P. E., E. R. Stein, S. D. Sevougian, L. J. Cunningham, J. M. Frederick, G. E. Hammond, T. S. Lowry, S. Jordan and E. Basurto (2018). Advances in Geologic Disposal Safety Assessment and an Unsaturated Alluvium Reference Case, SAND2018-11858 R. Albuquerque, NM, Sandia National Laboratories.

McNeil, M. B. and A. Odom (1994). Thermodynamic prediction of microbiologically influenced corrosion (MIC) by sulfate-reducing bacteria (SRB). Microbiologically influenced corrosion testing, ASTM International.

Pan G, AM Garde, and AR Atwood, in: Proceedings of LWR Fuel Performance Meeting TopFuel 2013, Charlotte, North Carolina, 15-19 September. American Nuclear Society.

Parkhurst, D. L. and C. A. J. Appelo (1999). User's guide to PHREEQC (Version 2) - A computer program for speciation, batch-reaction, one-dimensional transport, and inverse geochemical calculations. Water-Resources Investigations Report 99-4259. U.S. GEOLOGICAL SURVEY. Reston, VA.

Pescatore, C., M. Cowgill and T. Sullivan (1990). Zircaloy cladding performance under spent fuel disposal conditions, Brookhaven National Lab.

Price, L., A. Alsaed, P. Brady, F. Gelbard, V. Mousseau, M. Nole, J. Prouty, A. Salazar, K. Banerjee, S. Bhatt, G. Davidson, S. Painter, M. Swinney and E. Gonzalaez (2020). Status Report—Progress in Developing a Repository-Scale Performance Assessment Model.

Price, L. L., H. Alsaed, A. C. Barela, P. V. Brady, F. Gelbard, M. Gross, M. Nole, J. L. Prouty, K. Banerjee and S. Bhatt (2020). Preliminary Analysis of Postclosure DPC Criticality Consequences, Sandia National Lab.(SNL-NM), Albuquerque, NM (United States).

Shoesmith, D. W. (2013). "The chemistry/electrochemistry of spent nuclear fuel as a wasteform." Uranium: Cradle to Grave, Mineralogical Society of Canada, Short Course Series **43**: 337-368.

Siegmann, E. (2000). Clad Degradation - Summary and Abstraction ANL-WIS-MD-000007.

Siegmann, E. (2000). Initial cladding condition ANL-EBS-MD-000048 REV 00 ICN 01, YMP (Yucca Mountain Project, Las Vegas, Nevada).

Siegmann, E. (2004). Clad Degradation-FEPs Screening Arguments ANL-WIS-MD-000008 REV 00, Yucca Mountain Project, Las Vegas, Nevada (US).

SKB (Svensk Kärnbränslehantering AB) (2011). Long-term safety for the final repository for spent nuclear fuel at Forsmark. Main report of the SR-Site project Volume III.

Smith, H. (1988). Electrochemical corrosion-scoping experiments: An evaluation of the results, Westinghouse Hanford Co., Richland, WA (United States).

Stahl, D. (2005). Cladding Degradation Summary for LA. ANL-WIS-MD-000021 REV 03.

Tasooji, A., R. Einziger and A. Miller (1984). Modeling of zircaloy stress-corrosion cracking: texture effects and dry storage spent fuel behavior. Zirconium in the Nuclear Industry, ASTM International.

Westinghouse Electric Company LLC (2011). Westinghouse Technology Systems Manual, Section 3.1 Reactor Vessel and Internals, USNRC HRTD, REV 0909.

Yau, T. and R. Webster (1987). Corrosion of zirconium and hafnium. Metals handbook ninth edition. Volume 13. Corrosion.